A cerebellar thalamic cortical circuit for error-related cognitive control

Jaime S. Ide[1] and **Chiang-shan Ray Li**[1,2,3,*]

[1]Department of Psychiatry, Yale University School of Medicine, New Haven, CT 06519

[2]Department of Neurobiology, Yale University School of Medicine, New Haven, CT 06520

[3]Interdepartmental Neuroscience Program, Yale University School of Medicine, New Haven, CT 06520

Abstract

Error detection and behavioral adjustment are core components of cognitive control. Numerous studies have focused on the anterior cingulate cortex (ACC) as a critical locus of this executive function. Our previous work showed greater activation in the dorsal ACC and subcortical structures during error detection, and activation in the ventrolateral prefrontal cortex (VLPFC) during post-error slowing (PES) in a stop signal task (SST). However, the extent of error-related cortical or subcortical activation across subjects was not correlated with VLPFC activity during PES. So then, what causes VLPFC activation during PES? To address this question, we employed Granger causality mapping (GCM) and identified regions that Granger caused VLPFC activation in 54 adults performing the SST during fMRI. These brain regions, including the supplementary motor area (SMA), cerebellum, a pontine region, and medial thalamus, represent potential targets responding to errors in a way that could influence VLPFC activation. In confirmation of this hypothesis, the error-related activity of these regions correlated with VLPFC activation during PES, with the cerebellum showing the strongest association. The finding that cerebellar activation Granger causes prefrontal activity during behavioral adjustment supports a cerebellar function in cognitive control. Furthermore, multivariate GCA described the "flow of information" across these brain regions. Through connectivity with the thalamus and SMA, the cerebellum mediates error and post-error processing in accord with known anatomical projections. Taken together, these new findings highlight the role of the cerebello-thalamo-cortical pathway in an executive function that has heretofore largely been ascribed to the anterior cingulate-prefrontal cortical circuit.

Keywords

stop-signal task; conflict resolution; error detection; Granger causality; SMA; cerebellum

---

*Address correspondence to: Dr. Chiang-shan R. Li, Connecticut Mental Health Center, S112, Department of Psychiatry, Yale University School of Medicine, 34 Park Street, New Haven, CT 06519, Phone: 203-974-7354, FAX: 203-974-7076, chiang-shan.li@yale.edu.

Introduction

In our daily life, we constantly adjust our behavior by detecting changes in the environment and focusing on goal-relevant information. This ability, called cognitive control, is a hallmark of executive functions. One of the most influential neural models of cognitive control is the conflict-monitoring theory (Botvinick et al., 2001; Carter and van Veen, 2007; Ridderinkhof et al., 2004). This model posits that the anterior cingulate cortex (ACC) detects conflict and relays the information to prefrontal structures to expedite behavioral adjustment (Carter and van Veen, 2007). For instance, in a functional magnetic resonance imaging (fMRI) study of the Stroop task, Kerns et al. (2004) demonstrated that conflict-driven ACC activity predicts both prefrontal cortical activity and post-conflict behavioral adjustment in subsequent trials, lending support to the conflict-monitoring hypothesis. Behavioral adjustment in this study reflected primarily faster reaction time (RT) in an incongruent trial following an incongruent trial, compared to an incongruent trial following a congruent trial. It appears that incongruency-related activity in the ACC expedites the prefrontal processing of conflicting information and as a result shortens the RT during subsequent trials.

Errors often involve conflict. In our previous studies of the stop signal task (SST), we identified greater activation in the medial cortical areas, including dorsal ACC (dACC) during error detection (Li et al., 2008c), and the ventrolateral prefrontal cortex (VLPFC) during post-error slowing (PES) in go trial RT, an index of behavioral adjustment (Li et al., 2008b). However, across subjects, the extent of error-related cortical (including dACC) or subcortical activations was not correlated with VLPFC activity during PES (Li et al., 2008c). Along with other reports that did not show a correlation between error-related electrical potentials and post-error behavioral adjustment in event-related brain potential studies (Gehring and Fencsik, 2001; Riba et al., 2005), these results were at odds with the conflict monitoring hypothesis. However, these "negative" results led to an important question: what causes VLPFC activation during PES?

We attempted to address this question using Granger causality mapping (GCM, Roebroeck et al., 2005), a seed-based whole brain Granger Causality Analysis (GCA). GCA (Granger, 1969) is widely used in economics and finance research, and has been successfully applied to electroencephalographic and fMRI data to investigate the causal relationships between time series (Ding et al., 2000; Baccala and Sameshima, 2001; Goebel et al., 2003; Kaminski et al., 2001; Kus et al., 2004; Roebroeck et al., 2005). In fMRI, GCA has been used to examine effective connectivity between brain regions during cognitive performance (Abler et al., 2006; Deshpande et al., 2008; Duann et al., 2009; Sato et al., 2009; Stilla et al., 2008). In contrast to correlation based connectivity analyses, GCM elucidates directional functional connectivity between brain regions and would be a useful tool to explore this issue. We applied GCM to examine regions that influence VLPFC activity during the SST. Importantly, we anticipated that the error-related activation of some of these brain regions that Granger causes VLPFC would correlate with VLPFC activation during PES in linear regressions. Furthermore, we investigated the connectivities of these brain regions using multivariate GCA (Deshpande et al., 2009).

Material and methods

Behavioral task

We employed a simple reaction time task in this stop-signal paradigm (Li et al., 2006; 2008b; 2008a; Logan et al., 1984). There were two trial types: "go" and "stop," randomly intermixed. A small dot appeared on the screen to engage attention at the beginning of a go trial. After a randomized time interval (fore-period) between 1 and 5 s, the dot turned into a circle (the "go" signal), which served as an imperative stimulus, prompting the subjects to quickly press a

button. The circle vanished at a button press or after 1 s had elapsed, whichever came first, and the trial terminated. A premature button press prior to the appearance of the circle also terminated the trial. Three quarters of all trials were go trials. The remaining one quarter were stop trials. In a stop trial, an additional "X," the "stop" signal, appeared after and replaced the go signal. The subjects were told to withhold button press upon seeing the stop signal. Likewise, a trial terminated at button press or when 1 s had elapsed since the appearance of the stop signal. The stop signal delay (SSD) – the time interval between the go and stop signal – started at 200 ms and varied from one stop trial to the next according to a staircase procedure: if the subject succeeded in withholding the response, the SSD increased by 64 ms; conversely, if they failed, SSD decreased by 64 ms (Levitt, 1971). There was an inter-trial-interval of 2 s. Subjects were instructed to respond to the go signal quickly while keeping in mind that a stop signal could come up in a small number of trials. Prior to the fMRI study each subject had a practice session outside the scanner. In the scanner each subject completed four 10-min runs of the task with the SSD updated manually across runs. Depending on the actual stimulus timing (trials varied in fore-period duration) and speed of response, the total number of trials varied slightly across subjects in an experiment. With the staircase procedure we anticipated that the subjects would succeed in withholding their response in approximately half of the stop trials.

Subjects and MR imaging

We performed the study in fifty-four healthy subjects (27 men), who were all right-handed and between 22 and 45 years of age. They were paid to participate in the study and signed a written consent, after details of the study were explained, in accordance to guidelines and procedures approved by Yale University Human Investigation Committee.

Conventional T_1-weighted spin echo sagittal anatomical images were acquired for slice localization using a 3T scanner (Siemens Trio). Anatomical images of the functional slice locations were next obtained with spin echo imaging in the axial plane parallel to the AC-PC line with TR = 300 ms, TE = 2.5 ms, bandwidth = 300 Hz/pixel, flip angle = 60°, field of view = 220 × 220 mm, matrix = 256 × 256, 32 slices with slice thickness = 4mm and no gap. Functional, blood oxygenation level dependent (BOLD) signals were then acquired with a single-shot gradient echo echoplanar imaging (EPI) sequence. Thirty-two axial slices parallel to the AC-PC line covering the whole brain were acquired with TR = 2,000 ms, TE = 25 ms, trials occurred subsequent to and thus could not have a causal effect on the pSE trial (Li et al., 2008b). A statistical analytical design was constructed for each individual subject, using the general linear model (GLM) with the onsets of go signal in each of these trial types convolved with a canonical hemodynamic response function (HRF) and with the temporal derivative of the canonical HRF entered as regressors in the model (Friston et al., 1995). Realignment parameters in all six dimensions were also entered in the model. The data were high-pass filtered (128 s cutoff) to remove low-frequency signal drifts. Serial autocorrelation was corrected by a first-degree autoregressive or AR(1) model. In the first-level analysis, we constructed for each individual subject two contrasts: SE > G to isolate error-related activations, and pSEi > pSEni to isolate activations related to post-error slowing. We used MarsBaR to derive for each individual subject the effect size of activity change of these contrasts for regions of interest (Brett, 2002; http://marsbar.sourceforge.net/).

Methodological considerations for functional connectivity analysis

Investigation of the functional connectivities between brain regions is critical to our understanding of how information is integrated in the brain (Frackowiak et al., 2004; Friston, 1994; Penny et al., 2004; Stephan, 2004). For instance, structural equation modeling (SEM, Buchel and Friston, 1997; McIntosh and Gonzalez-Lima, 1994) and dynamic causal modeling (DCM, Friston et al., 2003) are widely used to test and compare competing models of neural networks. As pointed out by these and other investigators, limitations of SEM include its

requirement of an a priori anatomical model and assumption of unidirectional instantaneous connections (Buchel and Friston, 1997; Harrison et al., 2003; Penny et al., 2004). DCM is a generative model designed to fit fMRI data and has been successfully used in many studies (Friston et al., 2003; Penny et al., 2004; Stephan et al., 2009). DCM is particularly powerful in testing and comparing different patterns of effective connectivities. It is computationally demanding and its application is generally restricted to a limited number of ROIs (Penny et al., 2004). Psychophysiological interaction (PPI) is a voxel-wise analysis to examine whether correlation in activity between two brain bandwidth = 2004 Hz/pixel, flip angle = 85°, field of view = 220 × 220 mm, matrix = 64 × 64, 32 slices with slice thickness = 4mm and no gap. Three hundred images were acquired in each session.

Spatial preprocessing of brain images

Data were analyzed with Statistical Parametric Mapping version 5 (Wellcome Department of Imaging Neuroscience, University College London, U.K.). Images from the first five TRs at the beginning of each trial were discarded to enable the signal to achieve steady-state equilibrium between RF pulsing and relaxation. Images of each individual subject were first corrected for slice timing, realigned (motion-corrected) and unwarped (Andersson et al., 2001; Hutton et al., 2002). A mean functional image volume was constructed for each subject for each run from the realigned image volumes. These mean images were normalized to an MNI (Montreal Neurological Institute) EPI template with affine registration followed by nonlinear transformation (Ashburner and Friston, 1999). The normalization parameters determined for the mean functional volume were then applied to the corresponding functional image volumes for each subject. Finally, images were smoothed with a Gaussian kernel of 10 mm at Full Width at Half Maximum.

General Linear Modeling

Statistical modeling of the imaging data was described in detail in our earlier studies (Li et al., 2006; 2008b; 2008a). Briefly, four main types of trial outcome were first distinguished: go success (G), go error (F), stop success (SS), and stop error (SE) trial. G trials were divided into those that followed a G trial (pG), F trial (pF), SS trial (pSS), and SE trial (pSE), respectively (Li et al., 2008a). pSE trials (G trials that followed SE trial) were further divided into those that increased in RT (pSEi) and those that did not increase in RT (pSEni), to allow the isolation of neural processes involved in post-error behavioral adjustment (Li et al., 2008b). To determine whether a pSE trial increased or did not increase in RT, it was compared to the pG trials that preceded it in time during each session. The pG trials that followed the pSE trial were not included for comparison because the neural/cognitive processes associated with these pG areas is modulated by different psychological contexts (Friston et al., 1997; Gitelman et al., 2003). Because PPI analysis is based on the regression of instantaneous terms, it does not suggest direction of the connectivity (Friston et al., 1997).

Granger causality analysis (GCA, Granger, 1969) is a method of time series analysis and has been used to model temporal interaction of BOLD time series (Goebel et al., 2003; Roebroeck et al., 2005). Based on multivariate autoregressive modeling (Harrison et al., 2003), GCA has been applied to electroencephalographic and fMRI data to investigate the causal relationships between time series (Ding et al., 2000; Baccala and Sameshima, 2001; Kaminski et al., 2001; Kus et al., 2004; Roebroeck et al., 2005; Wilke et al., 2009) and to examine effective connectivity between brain regions during cognitive performance (Abler et al., 2006; Stilla et al., 2007; Deshpande et al., 2008; Duann et al., 2009; Sato et al., 2009). In contrast to correlation based connectivity analyses and PPI, GCA elucidates *directional* connectivity between brain regions. Therefore, in order to explore brain regions that provide *inputs* to the ventrolateral prefrontal cortex during stop signal performance, we employed GCA in the current study.

Granger Causality Analysis (GCA)

We employed multivariate autoregressive (MAR) modeling (Harrison et al., 2003; Sato et al., 2009) to perform GCA (Granger, 1969). In an unrestricted model of the BOLD time series

$$Y(t) = \sum_{i=1}^{p} A_i Y(t-i) + \varepsilon(t), \, t=1,2,\dots,T$$

(1)

$Y(t)$ is a column vector $[y_1(t), y_2(t),\dots,y_n(t)]$ in which each element $y_j(t)$, $j = 1,2,\dots n$, is the average time series of a region of interest (ROI) at time point t, T is the number of time points, n is the number of ROIs, and $\varepsilon(t)$ is a column vector $[\varepsilon_1(t), \varepsilon_2(t),\dots \varepsilon_n(t)]$ of residuals at time point t. The model order is represented by p and A_i is a n-by-n matrix given by

$$A_i = \begin{bmatrix} a_{11}^{(i)} & a_{12}^{(i)} & \cdots & a_{1n}^{(i)} \\ a_{21}^{(i)} & a_{22}^{(i)} & \cdots & a_{2n}^{(i)} \\ \vdots & \vdots & \ddots & \vdots \\ a_{n1}^{(i)} & a_{n2}^{(i)} & \cdots & a_{nn}^{(i)} \end{bmatrix}, \, i=1,2,\dots,p$$

(2)

estimated by ordinary least squares (Seth, 2010). To determine the model order we employed the Akaike Information Criterion (AIC), which trades the model-fit with a complexity penalty on the number of parameters (Akaike, 1974), which avoids over-fitting. The application of multivariate autoregressive modeling required that each ROI time series was covariance stationary, which we examined with the Augmented Dickey Fuller (ADF) test (Hamilton, 1994). ADF test verified that there was no unit root in the modeled time series. To test whether variable x Granger causes y, where $x, y \in Y(t)$, $x \neq y$, we computed the regression Equation (1) without variable x (the restricted model) and obtained the residual sum of squares RSS_r of variable y. The residual sum of squares of y is given by:

$RSS = \sum_{t=1}^{T} (y(t) - \widehat{y}(t))^2 = \sum_{t=1}^{T} \varepsilon(t)^2$, where $\hat{y}$ represents the predicted value of y. The influence from $x \rightarrow y$ can be measured by the fractional *F-value* (Hamilton, 1994):

$$F = \frac{(RSS_r - RSS_{ur}) \big/ p}{RSS_{ur} \big/ (T - 2p - 1)},$$

(3)

where RSS_{ur} is the residual sum of squares of variable y in the unrestricted model. Variable x causes y, if $F > F_{critical}$ (i.e., the inclusion of variable x significantly decreases the residual error).

An alternative connectivity measure used in the fMRI literature was proposed by Geweke (Geweke, 1982), in which linear dependence in the time domain from $x \rightarrow y$ (bivariate case) is measured by the expression (Geweke, 1982; Goebel et al., 2003):

$$F_{x \rightarrow y} = \ln \frac{\left| \text{var}(\varepsilon_y^*(t)) \right|}{\left| \text{var}(\varepsilon_y(t)) \right|},$$

(4)

where $\varepsilon_y(t)$ *is* the residual of variable y in the unrestricted model and $\varepsilon_y^*(t)$ is the residual of variable y in restricted model, i.e. autoregressive modeling without x variable. Equation (4)

can be extended to MAR by using the conditional linear dependence as the causality measure (Geweke, 1984; Chen et al., 2006; Seth, 2010). Analogously, variable x causes y, if $F_{x \to y} > F_{x \to y}$ (*critical*).

For statistical significance testing, the F-distribution can be used to compute the $F_{critical}$ of Equation (3), assuming independence of residuals, and χ^2-distribution can be employed to compute the $F_{x \to y}$(*critical*) of Equation (4) (Geweke, 1982; Bressler and Seth, in press). However, since MAR modeling potentially involves highly interdependent residuals (Deshpande et al., 2009), and there are no analytical statistical distributions for composed influence measures (Roebroeck et al., 2005), we employed a permutation resampling approach (Hesterberg et al., 2005; Seth, 2010) to test the causality measures. We computed empirical null distributions of *no causality* by producing surrogate data (Theiler et al., 1992) as implemented in previous EEG (Kaminski et al., 2001; Kus et al., 2004) and fMRI studies (Deshpande et al., 2009), and obtained the critical causality measures. The surrogate data was obtained by randomly generating time series with the same mean, variance, autocorrelation function, and spectrum as the original data (Theiler et al., 1992). Note that this constituted a permutation test because the original time series was resampled without replacement and the assumption of no causality was valid (Moore, 1999). In the surrogate data, the causal phase relationships were eliminated and significant connectivity occurred only by chance.

Whole-brain GCA or Granger Causality Mapping (GCM)

With GCM we examined which brain regions Granger-cause VLPFC (Goebel et al., 2003; Roebroeck et al., 2005). In this approach, the MAR model has two variables: a seed ROI, y, and the single voxel activity, x. GCM consists of computing the difference of influence measure ($F_{x \to y} - F_{y \to x}$) across the whole brain, i.e. $x \in X$, where X represents the set of brain voxels, and estimating its statistical significance. Equation (4) was used to compute the difference terms, as in Goebel et al. (2003). It was suggested that using the influence difference term ($F_{x \to y} - F_{y \to x}$), instead of $F_{x \to y}$, is more appropriate for inferring the unilateral connectivity x→y, because the difference term increases specificity (Roebroeck et al., 2005).

For each subject, the spatially preprocessed BOLD time series were averaged across all voxels inside the ROI. The average time series were concatenated across four sessions (each containing 295 time points) after linear detrending and normalization (subtraction of temporal mean and division by standard deviation) (Ding et al., 2000). The same de-trending and normalization procedures were executed for each voxel time series in the whole brain. We concatenated the average time series across four sessions in order to achieve covariance stationary time series. We did not consider the edge effects, since there were only 3 edges out of 1180 time points. We would also like to note that, alternatively, one could estimate a single MAR model from multiple sessions using the method of Ding et al. (2000), assuring that each session is an independent realization of a single statistically stationary process (Seth, 2010). We used the VLPFC mask as the seed ROI to compute the voxel-wise Granger causality map for all 54 subjects. That is, for each subject, we obtained a whole brain map of ($F_{x \to y} - F_{y \to x}$) values.

In group analysis for GCM, the *median* across subjects is used as group statistic and tested against an empirical null distribution, constructed using surrogate data (Theiler et al., 1992). For each single voxel in the brain (around 30,000 voxels in total), we tested the connectivity significance between the voxel and the selected ROI as follows: 1) we computed the median influence difference, $m = \overline{F_{x \to y} - F_{y \to x}}$, across 54 subjects; 2) constructed the empirical distribution of the null hypothesis (no connectivity), generating 500 samples of surrogate data per subject and calculating the average across 54 subjects; 3) estimated the corresponding $m_{critical}$ from the empirical distribution for a given p-value; and 4) compared m with the critical

value: if $m > m_{critical}$, we concluded that ROI (*y*) was caused by voxel *x*. As noted by Sato et al. (2009), the median across subjects is robust against outliers. Differently from Sato et al. (2009) which used resampled residuals, we employed surrogate data (Theiler et al., 1992) to produce the null distribution, as established in the EEG and fMRI literature (Kaminski et al., 2001; Kus et al., 2004; Deshpande et al., 2009).

Multivariate Granger Causality Analysis (GCA)

We employed multivariate GCA to further examine the connectivity among the ROIs that Granger caused VLPFC (Stilla et al., 2007; Deshpande et al., 2008; Deshpande et al., 2009). Multivariate GCA helps in identifying spurious influences between two structures x→y induced by common inputs from an unmodeled region z, x←z→y (Roebroeck et al., 2009). In particular, we tested the cortico-pontine cerebello-thalamic circuit by including: VLPFC, SMA, thalamus, pons, and cerebellum in one model. In a second model, we examined the connectivity without the pontine region (see below).

The multivariate GCA was performed for individual subjects. For each subject and each ROI, a summary time series was computed by averaging across voxels inside the ROI for each time point. As in GCM, these average time series were concatenated across sessions, after detrending and normalization (Ding et al., 2000). Afterwards, the five and four time series entered into MAR modeling (Equation (1)). In the case with five ROIs, one unrestricted MAR model and five restricted MAR models were estimated; and in the case with four ROIs, one unrestricted and four restricted models were estimated. Finally, the residual sums of squares (RSS) of restricted and unrestricted models were used to compute the measure of causality *F-values* (Equation (3)) for each possible connection. There were 20 and 12 possible connections each in the model with five and four ROIs. For each individual multivariate GCA, the optimal model order was estimated according to the unrestricted MAR model.

To obtain statistics for each connection, we generated 2,500 samples of surrogate data. For instance, in the model with five ROIs, each sample consisted of five random time series with the same spectrum of our original average time series. For each sample, we ran GCA and computed the *F-values* for each of the 20 possible connections, the distribution of which comprised the null hypothesis. Thus, $F_{critical}$ was estimated from the empirical distribution given a p-value. Finally, for each subject, we evaluated each of the possible connections, correcting for false discovery rate (FDR) in multiple comparisons (Genovese et al., 2002).

For multivariate GCA group analysis, we used binomial test to assess statistical significance (Uddin et al., 2009; Duann et al., 2009). For each connection, we counted the number of subjects that had $F > F_{critical}$ (i.e., significant connection, as described in the above) and estimated its significance using a binomial distribution with parameters $n = 54$ trials and $p = q = 0.5$ (same probability to observe a connection or not).

Results

Across 54 subjects performing the SST, the average go trial reaction time was 560.4±125.3ms and the critical SSD was 360.0±132.4ms. The go success rate was 95.9±4.3% and the stop success rate was 50.5±2.6%, suggesting that the staircase procedure was adequately tracking participants' performance.

With general linear modeling we examined regional brain activations associated with error occurrence and post-error slowing (PES) in RT during the stop signal task (Li et al., 2008b; Li et al., 2008c). The current results with 54 subjects confirmed our previous findings (Figure 1). Compared to G trials, stop error (SE) trials evoked greater activations in the medial frontal cortex (38,336mm³) including the dorsal anterior cingulate cortex (ACC; MNI coordinate x=4,

y=28, z=36, peak voxel Z=7.47) and the anterior supplementary motor area (SMA; MNI coordinates of two peaks: x=8, y=16, z=60, Z=7.08; and x=−4, y=16, z=48, Z=7.01), as well as the thalamus, epithalamus and structures in the midbrain (23,488mm^3 MNI coordinates of three peaks: x=4, y=−24, z=−4, Z=7.33; x=4; y=−16, z=−8, Z=7.16; and x=0; y=−20, z=−24, Z=6.34, respectively), p<0.05, corrected for family-wise error (FWE) of multiple comparisons. Compared to pSEni trials, pSEi trials evoked greater activation in the ventrolateral prefrontal cortex (VLPFC, MNI coordinate x=48, y=20, z=−8, Z=4.80, 1,536mm^3). Furthermore, the extent of error-related activity in the medial cortical or subcortical cluster was not correlated with VLPFC activity during PES across subjects (r=0.168 p=0.236; and r=0.181, p<0.190, respectively). To examine whether a significant correlation could be obtained of a more restricted area within these clusters, we also created regions of interest (ROIs), each of which was a sphere of 5mm in radius and centered on the coordinate of peak voxel activation. None of the six ROIs showed error-related activations that cross-correlated with VLPFC activation during post-error slowing (p's > 0.110).

We used Granger causality mapping (GCM) to explore brain regions that significantly influenced the VLPFC time series. The results of GCM identified the supplementary motor area (SMA), bilateral middle frontal cortices and precentral sulci, cerebellum (tonsil/vermis), a region near the pontine nuclei in the brain stem, and the medial thalamus (Figure 2 and Table 1). Note that this area of SMA partially overlapped the medial cortical cluster identified from GLM to respond to error; it was localized in a smaller and more posterior region (Figure 2, bottom inset).

We hypothesized that these brain regions would potentially respond to errors so to cause VLPFC activation during post-error slowing (PES). To examine this association, we computed the effect size of stop error (SE) > go success (G) for these regions of interest (ROIs) and correlated these error-related activities with VLPFC activation during PES across subjects. VLPFC activation was identified with a contrast between post-SE go trials with reaction time (RT) increase (pSEi) and post-SE go trials without RT increase (pSEni): pSEi > pSEni (Li et al., 2008b). We assumed Gaussian residuals and excluded three regression outliers using a confidence interval of 2.5% (Chatterjee and Hadi, 1986). The results confirmed our hypothesis with all except the pontine ROI (p=0.09132) showing a significant correlation and the cerebellum showing the strongest (Pearson r = 0.48386, p = 0.00032) correlation to VLPFC activation (Figure 3).

The simultaneous identification of the cerebellum, pons, medial thalamus, and SMA appeared particularly intriguing, as these brain regions were inter-connected anatomically (Kelly and Strick, 2003). We employed multivariate GCA to further characterize the connectivity in this cortico-ponto-cerebello-thalamo-cortical circuit and to distinguish direct and indirect connectivities between these regions. We evaluated the significance of each connection for individual subjects (p<0.05, corrected for false discovery rate, Genovese et al., 2002) and performed a binomial test in group analysis. This multivariate model failed to yield significant connectivity between the pontine and cerebellum ROIs (p's>0.44, binomial test). Note that the error-related activation of the pontine nuclei was also not correlated with VLPFC activation during PES. Thus, we included only the VLPFC, SMA, cerebellum, and thalamus in a second model. The results showed bilateral connectivity between the thalamus and the cerebellum as well as between the thalamus and the SMA, and unilateral projection from the thalamus as well as SMA to the VLPFC (Figure 4). The average optimal model order computed with AIC was 5.34, and the average (standard deviation) adjusted sum-squared-error was 0.41(±0.12), which was above the minimum of 0.3 as suggested by Seth (2010).

Discussion

Regional processes of post-error cognitive control

Using Granger causality mapping (GCM), we identified a medial cortical region, the supplementary motor area (SMA; MNI coordinate x=1; y=10; z=53), that responded to errors and correlated across subjects with ventrolateral prefrontal (VLPFC) activation during subsequent behavioral adjustment. The role of the SMA in error processing is broadly in accord with previous work demonstrating SMA activation in conflict resolution (Fiehler et al., 2004; Coxon et al., 2009), response competition (Hazeltine et al., 2000), and target or change detection (Linden et al., 1999). In particular, earlier recording studies of nonhuman primates described a role of supplementary eye field in performance monitoring and executive control during countermanding tasks (Schall et al., 2002; Stuphorn and Schall, 2006). Neurons in this brain region signal the production of errors and the presence of processing conflict (Schall et al., 2002).

In the current results, the medial cortical region that Granger caused VLPFC activation did not include the dorsal anterior cingulate cortex (dACC). Greater error-related activation was observed in general linear modeling (GLM) in a much larger cluster that involved both the dACC and SMA (Li et al., 2008b; see also the lower inset of Figure 2). We demonstrated that the average error-related activation of this medial cortical cluster or a more discrete region involving only the dACC did not correlate with the extent of PES or VLPFC activation during PES. Thus, while many previous studies supported a role of the dACC-prefrontal circuit for conflict-related cognitive control, the current findings appeared to suggest a SMA-prefrontal pathway for error-specific processes of cognitive control. The current findings are also consistent with an earlier neuropsychological study showing that dACC lesions did not impair PES during a go/no-go task in humans (Fellows and Farah, 2005). Interestingly, the broad area of SMA seemed to be spared in three of the four patients examined in this latter study. Overall, these results implicated a role of the SMA but not dACC in error-related cognitive control. Also of note is that this area of SMA did not overlap a more anterior region, which we labeled as anterior pre-SMA (MNI coordinate: x=−4; y=36; z=56) that our previous studies showed to mediate response inhibition in the stop signal task (Li et al., 2006; 2008a; Chao et al., 2009).

We observed activation in a small region of the medial thalamus that Granger caused VLPFC. This thalamic error-related activation positively correlated with VLPFC activation during PES. Many preclinical and clinical studies have suggested a role of the thalamus in performance monitoring, such as during matching sensory feedback with expected outcome of a motor response (Diamond and Ahissar, 2007; Urbain and Deschênes, 2007), re-evaluation of a reinforcer (Mitchell et al., 2007), task planning on the basis of external information (Wagner et al., 2006), processing corollary discharge of an eye movement (Sommer and Wurtz, 2004; Bellebaum et al., 2005), reception of negative feedback during the Wisconsin Card Sorting Task (Monchi et al., 2001), and self-generating actions in response to predictability of stimuli (Blakemore et al., 1998). Anatomical studies have consistently established a link between the mediodorsal thalamus and prefrontal cortices in humans as well as non-human primates (Yamamoto et al., 1992; Jones, 2002; Stepniewska et al., 2007).

Similarly, in our previous and current work we observed error-related activation in a region that covered almost the entire thalamus including the epithalamus and some structures in the midbrain (Li et al., 2008b). However, the error-related activation of this subcortical complex did not correlate linearly with VLPFC activation during PES. The current finding thus appeared to suggest a specific role of the mediodorsal thalamus but not other thalamic regions in error-related cognitive control.

The current results also showed that the cerebellar tonsil/vermis significantly Granger-caused VLPFC during the stop signal task, with its error-related activity strongly correlated with VLPFC activation during PES. Cerebellar tonsils along with the vermis make up the spinocerebellum (Orrison, 2008). The tonsil receives its input from the spinocerebellar tracts, and influences limb movement and posture through descending projections from the globose and fastigial nuclei (Orrison, 2008). The cerebellum has long been implicated in motor control, and it was hypothesized in recent literature to mediate non-motor, including cognitive, functioning (see Ito, 2008 for an overview). For instance, cerebellar tonsil and posterior vermis were engaged in attention processing in a motor task (Allen et al., 1997), verbal working memory (Desmond et al., 1997), motor imagery (Ross et al., 2003), spatial attention (Mayer et al., 2007), motor coordination and timing learning (Kim et al., 2008), and retinal coding of target velocity (Nagel et al., 2008).

Providing evidence for error-related cerebellar activation that Granger caused prefrontal activity during behavioral adjustment, the current findings thus implicate cerebellum specifically in cognitive control, consistent with many previous studies (Middleton and Strick, 1994; Ramnani, 2006; Hayter et al., 2007; Thach, 2007). For instance, Schweizer and colleagues observed that patients with chronic focal cerebellum lesions but intact prefrontal cortex were slower and less accurate in a task-switching task involving conflict resolution, compared to healthy controls (Schweizer et al., 2007). These "cerebellar patients" performed normally in a task without response conflict, suggesting an indispensable role of the cerebellum in conflict (of which error is oftentimes a consequence) related cognitive processing. In imaging studies, Broekhoven and colleagues observed greater activation of the cerebellar vermis and lobules during saccadic errors (van Broekhoven et al., 2009); Tanaka and colleagues demonstrated greater premotor cortical and cerebellar activations during error correcting movements in a force production task, with the cerebellum figuring dominantly in error correction during slow and well-controlled movements (Tanaka et al., 2009). Taken together, along with these earlier studies, the current findings support a cerebellar function in cognitive control.

An important question is why we did not observe error-related cerebellar activation on the basis of GLM. As shown in Figure 3, more subjects show a negative than positive BOLD contrast for stop error versus go trials in the cerebellar cluster. Thus, cerebellum would not demonstrate significant error-related activity across the entire sample of subjects on the basis of GLM. This observation speaks to a critical issue in differential imaging or the use of "cognitive subtraction" in fMRI (Friston et al., 1996; Logothetis, 2008). That is, by contrasting two β's from the GLM and labeling the difference as specific to a psychological construct (error, in this case), one would have to assume that all other constructs are equally represented in the two β's, an assumption that all too often is not valid (Friston et al., 1996). For instance, one might speculate that stimulus or error processing interacted with motor response in stop error (SE) trials such that the motor processes elicited significantly less activation in the cerebellum during SE as compared to go trials. In a contrast between SE and go trials, the cerebellum exhibited a range of activations with a mean that could not be detected with GLM. Without this limitation, thus, GCM seems to provide a useful tool to uncover functional connectivity that in turn helps elucidate the functions of individual brain regions.

A cerebello-thalamo-cortical circuit for error-related cognitive control

Anatomical studies in non-human primates have long documented connections between cerebral cortical structures and the cerebellar cortex via the cortico-ponto-cerebellar and cerebello-thalamocortical pathways (Brodal, 1978; Schmahmann and Pandya, 1997). The cerebello-thalamocortical projections involve not only the primary motor cortex (Evarts and Thach, 1969; Allen and Tsukahara, 1974) but also non-motor cortical areas (Middleton and

Strick, 1994; Percheron et al., 1996) as targets, implicating this circuit in non-motor functions. Functional connectivity between cerebellum and prefrontal cortices were shown recently in humans during resting state and during performance of a cognitive task (Allen et al., 2005; Demirci et al., 2009; Lin et al., 2009). Furthermore, diffusion tensor imaging tractography demonstrated cerebellar projections to the prefrontal cortex via the thalamus in humans (Jissendi et al., 2008). Overall, both anatomical and functional imaging studies have provided abundant evidence in support of the cerebello-thalamocortical circuit for various motor and cognitive operations.

GCM identified a region in or near the pontine nucleus that significantly Granger caused VLPFC time series. Thus, these findings appeared to indicate a role of the cortico-ponto-cerebello-thalamic circuit in mediating error-related cognitive control, in accord with known anatomical projections in human and non-human primates (Kelly and Strick, 2003). We performed multivariate GCA to explore the functional connectivity across these brain regions during error and post-error processing. An initial model with the VLPFC, cerebellum, pons, medial thalamus, and SMA as regions of interest did not yield any significant connections between the pons and cerebellum. We thus did not have evidence for a functional cortico-ponto-cerebello-thalamo-cortical circuit during error and post-error processing in the stop signal task. It is also worth noting that, unlike cerebellum, medial thalamus, and the SMA, error-related activation of the pontine region did not significantly correlate with VLPFC activation during PES. In a second multivariate GCA, we explored the connectivity between the VLPFC, cerebellum, thalamus, and SMA. The results suggested bilateral connections between the cerebellum and thalamus and between the thalamus and the SMA, as well as unilateral projection from the thalamus to the VLPFC and from the SMA to the VLPFC. In no case did the VLPFC Granger cause the other structures. Although one is cautioned not to over-interpret the strength of the connections, we feel that the pattern of functional connectivities observed in this model is consistent with extant knowledge of the anatomy and function of the cerebello-thalamocortical circuits (Ramnani, 2006).

Methodological considerations and limitations of GCA

Friston et al. 2009 discussed a number of disadvantages of GCA, while Roebroeck et al., 2009 debated the importance of causality concepts based on temporal precedence (such as Granger causality) in connectivity analysis. For instance, GCA does not involve modulation of the connectivity by experimental conditions, as does PPI analysis. Thus, GCA alone does not guarantee "causality" between regional brain activations in response to specific events in the cognitive task. Additionally, as described in the Methods, bivariate connectivity measures such as Granger causality mapping (GCM) are susceptible to confound by large network interactions (Roebroeck et al., 2005). Two brain areas (voxels) could appear to be connected only because they receive a common input from a third area (voxel).

Another methodological issue in GCA concerns the slow, variable and unknown hemodynamic responses. GCA relies on the temporal information provided by the measured BOLD signal and is susceptible to the filtering of the neuronal response by the hemodynamic response function (HRF) and the down-sampling of the BOLD signal. As a result, it could lead to spurious connectivity between two brain regions (Kayser et al., 2009; Roebroeck et al., 2005). On the other hand, analyses of fMRI data obtained in a motor task showed that, although GCM results were not entirely consistent in individual subjects, a significant pattern of directional connectivity could be obtained for the whole group (Kayser et al., 2009). The authors argued that, assuming that there is no reliable relationship across subjects in the hemodynamic response profile between different brains areas, consistent findings from group analysis should reflect neural rather than HRF differences (Kayser et al., 2009).

In a recent report of simultaneous EEG and fMRI recordings in rats, in which HRFs were individually estimated, David et al., 2008 showed that the deconvolved BOLD signals are important for GCA to identify correct neuronal connections. Minimizing the effects of HRF variability using explicit (Glover, 1999; Chang et al., 2008) or implicit (such as in DCM) deconvolution techniques seems to contribute to the success of connectivity analyses including GCA of fMRI data (David et al, 2008). However, the success of deconvolution depends on correct estimation of the HRF across the brain, which is not a trivial task (Roebroeck et al., 2009).

We recognized these limitations and employed GCM only to identify target brain regions that may cause prefrontal activation during post-error slowing (PES). Whether error-related activation of these brain regions is associated with prefrontal activity during PES is tested and confirmed by linear correlation across the entire sample of subjects. Furthermore, we employed multivariate GCA to elucidate the interaction between these brain regions. The results seemed to accord with known anatomy, with the caveat that a significant connection does not imply direct causality.

Conclusions and implications

In our previous work, we identified the ventrolateral prefrontal cortex (VLPFC) as the neural correlate of post-error slowing (PES) during a stop-signal task (SST, Li et al., 2008b). Using Granger causality mapping (GCM) here, we identified regions in the cerebellum, thalamus, and supplementary motor area (SMA), whose error-related activation cross-correlated with VLPFC activation during PES. In addition, the results from the multivariate GCA indicated a putative cerebello-thalamocortical circuit that mediates error processing and PES during the SST. This study thus complemented the literature by presenting novel findings on the neural processes of error-related cognitive control. The current findings also provided evidence for the utility of the GCA in identifying brain structures whose role in cognitive performance might elude general linear modeling and in elucidating the neural circuit mediating the performance. Finally, the role of the cerebello-thalamocortical circuit in cognitive control may have implications for our research of the etiology of some common neurological conditions such as attention deficit hyperactivity disorder (Schulz et al., 2004; Bush et al., 2005; Wolf et al., 2009).

Research Highlights

- Error-related ACC activation is not associated with post-error prefrontal activation

- Regions Granger-causing VLPFC activation

- Cerebello-thalamo-cortical circuit causes prefrontal activation in cognitive control

Acknowledgments

References

Abler B, Roebroeck A, Goebel R, Hose A, Schonfeldt-Lecuona C, Hole G, Walter H. Investigating directed influences between activated brain areas in a motor-response task using fMRI. Magn Reson Imaging 2006;24:181–185. [PubMed: 16455407]

Akaike H. A new look at the statistical model identification. Automatic Control, IEEE Transactions on 1974;19:723.

Allen G, Buxton RB, Wong EC, Courchesne E. Attentional activation of the cerebellum independent of motor involvement. Science 1997;275:1940–1943. [PubMed: 9072973]

Allen G, McColl R, Barnard H, Ringe WK, Fleckenstein J, Cullum CM. Magnetic resonance imaging of cerebellar-prefrontal and cerebellar-parietal functional connectivity. Neuroimage 2005;28:39–48. [PubMed: 16023375]

Allen GI, Tsukahara N. Cerebrocerebellar communication systems. Physiol Rev 1974;54:957–1006. [PubMed: 4370744]

Andersson JL, Hutton C, Ashburner J, Turner R, Friston K. Modeling geometric deformations in EPI time series. Neuroimage 2001;13:903–919. [PubMed: 11304086]

Ashburner J, Friston KJ. Nonlinear spatial normalization using basis functions. Hum Brain Mapp 1999;7:254–266. [PubMed: 10408769]

Baccala LA, Sameshima K. Partial directed coherence: a new concept in neural structure determination. Biol Cybern 2001;84:463–474. [PubMed: 11417058]

Bellebaum C, Daum I, Koch B, Schwarz M, Hoffmann KP. The role of the human thalamus in processing corollary discharge. Brain 2005;128:1139–1154. [PubMed: 15758033]

Blakemore SJ, Rees G, Frith CD. How do we predict the consequences of our actions? A functional imaging study. Neuropsychologia 1998;36:521–529. [PubMed: 9705062]

Botvinick MM, Braver TS, Barch DM, Carter CS, Cohen JD. Conflict monitoring and cognitive control. Psychol Rev 2001;108:624–652. [PubMed: 11488380]

Bressler SL, Tang W, Sylvester CM, Shulman GL, Corbetta M. Top-down control of human visual cortex by frontal and parietal cortex in anticipatory visual spatial attention. J Neurosci 2008;28:10056–10061. [PubMed: 18829963]

Bressler SL, Seth AK. Wiener-Granger Causality: A well established methodology. Neuroimage. (in press).

Brett, M.; Anton, JL.; Valabregue, R.; Poline, JB. Region of interest analysis using an SPM toolbox (abstract). 8th International Conference on Functional Mapping of the Human Brain; Sendai, Japan: 2002.

Brodal P. The corticopontine projection in the rhesus monkey. Origin and principles of organization. Brain 1978;101:251–283. [PubMed: 96910]

Buchel C, Friston KJ. Modulation of connectivity in visual pathways by attention: cortical interactions evaluated with structural equation modelling and fMRI. Cereb Cortex 1997;7:768–778. [PubMed: 9408041]

Bush G, Valera EM, Seidman LJ. Functional neuroimaging of attention-deficit/hyperactivity disorder: a review and suggested future directions. Biol Psychiatry 2005;57:1273–1284. [PubMed: 15949999]

Carter CS, van Veen V. Anterior cingulate cortex and conflict detection: an update of theory and data. Cogn Affect Behav Neurosci 2007;7:367–379. [PubMed: 18189010]

Chang C, Thomason ME, Glover GH. Mapping and correction of vascular hemodynamic latency in the BOLD signal. Neuroimage 2008;43:90–102. [PubMed: 18656545]

Chao HH, Luo X, Chang JL, Li CS. Activation of the pre-supplementary motor area but not inferior prefrontal cortex in association with short stop signal reaction time - an intra-subject analysis. BMC Neurosci 2009;10:75. [PubMed: 19602259]

Chatterjee S, Hadi AS. Influential observations, high leverage points, and outliers in linear regression. Stat Science 1986;1:379.

Chen Y, Bressler SL, Ding M. Frequency decomposition of conditional Granger causality and application to multivariate neural field potential data. J Neurosci Methods 2006;150:228–237. [PubMed: 16099512]

Coxon JP, Stinear CM, Byblow WD. Stop and go: the neural basis of selective movement prevention. J Cogn Neurosci 2009;21:1193–1203. [PubMed: 18702592]

David O, Guillemain I, Saillet S, Reyt S, Deransart C, Segebarth C, Depaulis A. Identifying neural drivers with functional MRI: an electrophysiological validation. PLoS Biol 2008;6:2683–2697. [PubMed: 19108604]

Demirci O, Stevens MC, Andreasen NC, Michael A, Liu J, White T, Pearlson GD, Clark VP, Calhoun VD. Investigation of relationships between fMRI brain networks in the spectral domain using ICA and Granger causality reveals distinct differences between schizophrenia patients and healthy controls. Neuroimage 2009;46:419–431. [PubMed: 19245841]

Deshpande G, Hu X, Stilla R, Sathian K. Effective connectivity during haptic perception: a study using Granger causality analysis of functional magnetic resonance imaging data. Neuroimage 2008;40:1807–1814. [PubMed: 18329290]

Deshpande G, LaConte S, James GA, Peltier S, Hu X. Multivariate Granger causality analysis of fMRI data. Hum Brain Mapp 2009;30:1361–1373. [PubMed: 18537116]

Desmond JE, Gabrieli JD, Wagner AD, Ginier BL, Glover GH. Lobular patterns of cerebellar activation in verbal working-memory and finger-tapping tasks as revealed by functional MRI. J Neurosci 1997;17:9675–9685. [PubMed: 9391022]

Diamond ME, Ahissar E. When outgoing and incoming signals meet: new insights from the zona incerta. Neuron 2007;56:578–579. [PubMed: 18031676]

Ding M, Bressler SL, Yang W, Liang H. Short-window spectral analysis of cortical event-related potentials by adaptive multivariate autoregressive modeling: data preprocessing, model validation, and variability assessment. Biol Cybern 2000;83:35–45. [PubMed: 10933236]

Duann JR, Ide JS, Luo X, Li CS. Functional connectivity delineates distinct roles of the inferior frontal cortex and presupplementary motor area in stop signal inhibition. J Neurosci 2009;29:10171–10179. [PubMed: 19675251]

Evarts EV, Thach WT. Motor mechanisms of the CNS: cerebrocerebellar interrelations. Annu Rev Physiol 1969;31:451–498. [PubMed: 4885774]

Fellows LK, Farah MJ. Is anterior cingulate cortex necessary for cognitive control? Brain 2005;128:788–796. [PubMed: 15705613]

Fiehler K, Ullsperger M, von Cramon DY. Neural correlates of error detection and error correction: is there a common neuroanatomical substrate? Eur J Neurosci 2004;19:3081–3087. [PubMed: 15182316]

Frackowiak, R.; Ashburner, J.; Penny, W.; Zeki, S. Human Brain Function. Second Edition. Academic Press; 2004.

Friston K. Functional and effective connectivity in neuroimaging: A synthesis. Human Brain Mapping 1994;2:78.

Friston KJ, Ashburner J, Frith CD, Poline JB, Heather JD, Frackowiak RSJ. Spatial registration and normalization of images. Human Brain Mapping 1995;3:165–189.

Friston KJ, Price CJ, Fletcher P, Moore C, Frackowiak RS, Dolan RJ. The trouble with cognitive subtraction. Neuroimage 1996;4:97–104. [PubMed: 9345501]

Friston KJ, Buechel C, Fink GR, Morris J, Rolls E, Dolan RJ. Psychophysiological and modulatory interactions in neuroimaging. Neuroimage 1997;6:218–229. [PubMed: 9344826]

Friston KJ, Harrison L, Penny W. Dynamic causal modelling. NeuroImage 2003;19:1273. [PubMed: 12948688]

Friston K. Causal modelling and brain connectivity in functional magnetic resonance imaging. PLoS Biol 2009;7:e1000033.

Gehring WJ, Fencsik DE. Functions of the medial frontal cortex in the processing of conflict and errors. J Neurosci 2001;21:9430–9437. [PubMed: 11717376]

Genovese CR, Lazar NA, Nichols T. Thresholding of statistical maps in functional neuroimaging using the false discovery rate. Neuroimage 2002;15:870–878. [PubMed: 11906227]

Geweke J. Measurement of linear dependence and feedback between multiple time series. J Am Stat Ass 1982;77:313.

Geweke JF. Measures of Conditional Linear Dependence and Feedback Between Time Series. Journal of the American Statistical Association 1984;79:907.

Gitelman DR, Penny WD, Ashburner J, Friston KJ. Modeling regional and psychophysiologic interactions in fMRI: the importance of hemodynamic deconvolution. Neuroimage 2003;19:200–207. [PubMed: 12781739]

Glover GH. Deconvolution of impulse response in event-related BOLD fMRI. Neuroimage 1999;9:416–429. [PubMed: 10191170]

Goebel R, Roebroeck A, Kim DS, Formisano E. Investigating directed cortical interactions in time-resolved fMRI data using vector autoregressive modeling and Granger causality mapping. Magn Reson Imaging 2003;21:1251–1261. [PubMed: 14725933]

Granger CWJ. Investigating Causal Relations by Econometric Models and Cross-spectral Methods. Econometrica 1969;37:424.

Hamilton, JD. Time Series Analysis. Princeton, NJ: Princeton University Press; 1994.

Harrison L, Penny WD, Friston K. Multivariate autoregressive modeling of fMRI time series. Neuroimage 2003;19:1477–1491. [PubMed: 12948704]

Hayter AL, Langdon DW, Ramnani N. Cerebellar contributions to working memory. Neuroimage 2007;36:943–954. [PubMed: 17468013]

Hazeltine E, Poldrack R, Gabrieli JD. Neural activation during response competition. J Cogn Neurosci 2000;12 Suppl 2:118–129. [PubMed: 11506652]

Hesterberg, T.; Moore, DS.; Monaghan, S.; Clipson, A.; R, E. Bootstrap methods and permutation tests. In: Moore, DSGPM., editor. Introduction to the Practice of Statistics. 5th Edition. New York: WH Freeman & Co; 2005. p. 14.11-14.70.

Hutton C, Bork A, Josephs O, Deichmann R, Ashburner J, Turner R. Image distortion correction in fMRI: A quantitative evaluation. Neuroimage 2002;16:217–240. [PubMed: 11969330]

Ito M. Control of mental activities by internal models in the cerebellum. Nat Rev Neurosci 2008;9:304–313. [PubMed: 18319727]

Jissendi P, Baudry S, Baleriaux D. Diffusion tensor imaging (DTI) and tractography of the cerebellar projections to prefrontal and posterior parietal cortices: a study at 3T. J Neuroradiol 2008;35:42–50. [PubMed: 18206240]

Jones EG. Thalamic circuitry and thalamocortical synchrony. Philos Trans R Soc Lond B Biol Sci 2002;357:1659–1673. [PubMed: 12626002]

Kaminski M, Ding M, Truccolo WA, Bressler SL. Evaluating causal relations in neural systems: granger causality, directed transfer function and statistical assessment of significance. Biol Cybern 2001;85:145–157. [PubMed: 11508777]

Kayser AS, Sun FT, D'Esposito M. A comparison of Granger causality and coherency in fMRI-based analysis of the motor system. Hum Brain Mapp 2009;30:3475–3494. [PubMed: 19387980]

Kelly RM, Strick PL. Cerebellar loops with motor cortex and prefrontal cortex of a nonhuman primate. J Neurosci 2003;23:8432–8444. [PubMed: 12968006]

Kerns JG, Cohen JD, MacDonald AW 3rd, Cho RY, Stenger VA, Carter CS. Anterior cingulate conflict monitoring and adjustments in control. Science 2004;303:1023–1026. [PubMed: 14963333]

Kim J, Lee HM, Kim WJ, Park HJ, Kim SW, Moon DH, Woo M, Tennant LK. Neural correlates of pre-performance routines in expert and novice archers. Neurosci Lett 2008;445:236–241. [PubMed: 18805460]

Kus R, Kaminski M, Blinowska KJ. Determination of EEG activity propagation: pair-wise versus multichannel estimate. IEEE Trans Biomed Eng 2004;51:1501–1510. [PubMed: 15376498]

Levitt H. Transformed up-down methods in psychoacoustics. J Acoust Soc Am 1971;49 Suppl 2:467+. [PubMed: 5541744]

Li CS, Huang C, Constable RT, Sinha R. Imaging response inhibition in a stop-signal task: neural correlates independent of signal monitoring and post-response processing. J Neurosci 2006;26:186–192. [PubMed: 16399686]

Li CS, Yan P, Sinha R, Lee TW. Subcortical processes of motor response inhibition during a stop signal task. Neuroimage 2008a;41:1352–1363. [PubMed: 18485743]

Li CS, Huang C, Yan P, Paliwal P, Constable RT, Sinha R. Neural correlates of post-error slowing during a stop signal task: a functional magnetic resonance imaging study. J Cogn Neurosci 2008b;20:1021–1029. [PubMed: 18211230]

Li CS, Yan P, Chao HH, Sinha R, Paliwal P, Constable RT, Zhang S, Lee TW. Error-specific medial cortical and subcortical activity during the stop signal task: a functional magnetic resonance imaging study. Neuroscience 2008c;155:1142–1151. [PubMed: 18674592]

Lin FH, Agnew JA, Belliveau JW, Zeffiro TA. Functional and effective connectivity of visuomotor control systems demonstrated using generalized partial least squares and structural equation modeling. Hum Brain Mapp 2009;30:2232–2251. [PubMed: 19288462]

Linden DE, Prvulovic D, Formisano E, Vollinger M, Zanella FE, Goebel R, Dierks T. The functional neuroanatomy of target detection: an fMRI study of visual and auditory oddball tasks. Cereb Cortex 1999;9:815–823. [PubMed: 10601000]

Logan GD, Cowan WB, Davis KA. On the ability to inhibit simple and choice reaction time responses: a model and a method. J Exp Psychol Hum Percept Perform 1984;10:276–291. [PubMed: 6232345]

Logothetis NK. What we can do and what we cannot do with fMRI. Nature 2008;453:869–878. [PubMed: 18548064]

Mayer AR, Harrington DL, Stephen J, Adair JC, Lee RR. An event-related fMRI Study of exogenous facilitation and inhibition of return in the auditory modality. J Cogn Neurosci 2007;19:455–467. [PubMed: 17335394]

McIntosh AR, Gonzalez-Lima F. Structural equation modeling and its application to network analysis in functional brain imaging. Human Brain Mapping 1994;2:2–22.

Middleton FA, Strick PL. Anatomical evidence for cerebellar and basal ganglia involvement in higher cognitive function. Science 1994;266:458–461. [PubMed: 7939688]

Mitchell AS, Browning PG, Baxter MG. Neurotoxic lesions of the medial mediodorsal nucleus of the thalamus disrupt reinforcer devaluation effects in rhesus monkeys. J Neurosci 2007;27:11289–11295. [PubMed: 17942723]

Moore JH. Bootstrapping, permutation testing and the method of surrogate data. Physics in Medicine and Biology 1999;44:L11. [PubMed: 10498505]

Monchi O, Petrides M, Petre V, Worsley K, Dagher A. Wisconsin Card Sorting revisited: distinct neural circuits participating in different stages of the task identified by event-related functional magnetic resonance imaging. J Neurosci 2001;21:7733–7741. [PubMed: 11567063]

Nagel M, Sprenger A, Hohagen F, Binkofski F, Lencer R. Cortical mechanisms of retinal and extraretinal smooth pursuit eye movements to different target velocities. Neuroimage 2008;41:483–492. [PubMed: 18420428]

Orrison, WW. Atlas of Brain Function. 2nd Edition. New York: Thieme; 2008.

Penny WD, Stephan KE, Mechelli A, Friston KJ. Modelling functional integration: a comparison of structural equation and dynamic causal models. Neuroimage 2004;23 Suppl 1:S264–S274. [PubMed: 15501096]

Percheron G, Francois C, Talbi B, Yelnik J, Fenelon G. The primate motor thalamus. Brain Res Brain Res Rev 1996;22:93–181. [PubMed: 8883918]

Ramnani N. The primate cortico-cerebellar system: anatomy and function. Nat Rev Neurosci 2006;7:511–522. [PubMed: 16791141]

Riba J, Rodriguez-Fornells A, Munte TF, Barbanoj MJ. A neurophysiological study of the detrimental effects of alprazolam on human action monitoring. Brain Res Cogn Brain Res 2005;25:554–565. [PubMed: 16168630]

Ridderinkhof KR, van den Wildenberg WP, Segalowitz SJ, Carter CS. Neurocognitive mechanisms of cognitive control: the role of prefrontal cortex in action selection, response inhibition, performance monitoring, and reward-based learning. Brain Cogn 2004;56:129–140. [PubMed: 15518930]

Roebroeck A, Formisano E, Goebel R. Mapping directed influence over the brain using Granger causality and fMRI. Neuroimage 2005;25:230–242. [PubMed: 15734358]

Roebroeck A, Formisano E, Goebel R. The identification of interacting networks in the brain using fMRI: Model selection, causality and deconvolution. Neuroimage. 2009

Ross JS, Tkach J, Ruggieri PM, Lieber M, Lapresto E. The mind's eye: functional MR imaging evaluation of golf motor imagery. AJNR Am J Neuroradiol 2003;24:1036–1044. [PubMed: 12812924]

Sato JR, Takahashi DY, Arcuri SM, Sameshima K, Morettin PA, Baccala LA. Frequency domain connectivity identification: an application of partial directed coherence in fMRI. Hum Brain Mapp 2009;30:452–461. [PubMed: 18064582]

Schall JD, Stuphorn V, Brown JW. Monitoring and control of action by the frontal lobes. Neuron 2002;36:309–322. [PubMed: 12383784]

Schmahmann JD, Pandya DN. Anatomic organization of the basilar pontine projections from prefrontal cortices in rhesus monkey. J Neurosci 1997;17:438–458. [PubMed: 8987769]

Schulz KP, Fan J, Tang CY, Newcorn JH, Buchsbaum MS, Cheung AM, Halperin JM. Response inhibition in adolescents diagnosed with attention deficit hyperactivity disorder during childhood: an event-related FMRI study. Am J Psychiatry 2004;161:1650–1657. [PubMed: 15337656]

Schweizer TA, Oriet C, Meiran N, Alexander MP, Cusimano M, Stuss DT. The cerebellum mediates conflict resolution. J Cogn Neurosci 2007;19:1974–1982. [PubMed: 17892387]

Seth AK. A MATLAB toolbox for Granger causal connectivity analysis. J Neurosci Methods 2010;186:262–273. [PubMed: 19961876]

Sommer MA, Wurtz RH. What the brain stem tells the frontal cortex. II. Role of the SC-MD-FEF pathway in corollary discharge. J Neurophysiol 2004;91:1403–1423. [PubMed: 14573557]

Stephan KE. On the role of general system theory for functional neuroimaging. J Anat 2004;205:443–470. [PubMed: 15610393]

Stephan KE, Penny WD, Daunizeau J, Moran RJ, Friston KJ. Bayesian model selection for group studies. Neuroimage 2009;46:1004–1017. [PubMed: 19306932]

Stepniewska I, Preuss TM, Kaas JH. Thalamic connections of the dorsal and ventral premotor areas in New World owl monkeys. Neuroscience 2007;147:727–745. [PubMed: 17570597]

Stilla R, Deshpande G, LaConte S, Hu X, Sathian K. Posteromedial parietal cortical activity and inputs predict tactile spatial acuity. J Neurosci 2007;27:11091–11102. [PubMed: 17928451]

Stuphorn V, Schall JD. Executive control of countermanding saccades by the supplementary eye field. Nat Neurosci 2006;9:925–931. [PubMed: 16732274]

Tanaka Y, Fujimura N, Tsuji T, Maruishi M, Muranaka H, Kasai T. Functional interactions between the cerebellum and the premotor cortex for error correction during the slow rate force production task: an fMRI study. Exp Brain Res 2009;193:143–150. [PubMed: 19139866]

Thach WT. On the mechanism of cerebellar contributions to cognition. Cerebellum 2007;6:163–167. [PubMed: 17786811]

Theiler J, Eubank S, Longtin A, Galdrikian B, Doyne. Testing for nonlinearity in time series: the method of surrogate data. Physica D: Nonlinear Phenomena 1992;58:77–94.

Uddin LQ, Kelly AM, Biswal BB, Xavier Castellanos F, Milham MP. Functional connectivity of default mode network components: correlation, anticorrelation, and causality. Hum Brain Mapp 2009;30:625–637. [PubMed: 18219617]

Urbain N, Deschênes M. Motor cortex gates vibrissal responses in a thalamocortical projection pathway. Neuron 2007;56:714–725. [PubMed: 18031687]

van Broekhoven PC, Schraa-Tam CK, van der Lugt A, Smits M, Frens MA, van der Geest JN. Cerebellar Contributions to the Processing of Saccadic Errors. Cerebellum. 2009

Wagner G, Koch K, Reichenbach JR, Sauer H, Schlosser RG. The special involvement of the rostrolateral prefrontal cortex in planning abilities: an event-related fMRI study with the Tower of London paradigm. Neuropsychologia 2006;44:2337–2347. [PubMed: 16806311]

Wetherill GB, Chen H, Vasudeva RB. Sequential estimation of quantal response curves: A new method of estimation. Biometrika 1966;53:439–454.

Wilke M, Lidzba K, Krageloh-Mann I. Combined functional and causal connectivity analyses of language networks in children: a feasibility study. Brain Lang 2009;108:22–29. [PubMed: 18952275]

Wolf RC, Plichta MM, Sambataro F, Fallgatter AJ, Jacob C, Lesch KP, Herrmann MJ, Schonfeldt-Lecuona C, Connemann BJ, Gron G, Vasic N. Regional brain activation changes and abnormal functional connectivity of the ventrolateral prefrontal cortex during working memory processing in adults with attention-deficit/hyperactivity disorder. Hum Brain Mapp 2009;30:2252–2266. [PubMed: 19107748]

Yamamoto T, Yoshida K, Yoshikawa H, Kishimoto Y, Oka H. The medial dorsal nucleus is one of the thalamic relays of the cerebellocerebral responses to the frontal association cortex in the monkey: horseradish peroxidase and fluorescent dye double staining study. Brain Res 1992;579:315–320. [PubMed: 1378349]
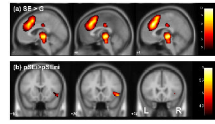
Figure 1.
(a) The medial frontal cortex, including the dorsal anterior cingulate cortex and supplementary motor area, as well as a cluster that includes the thalamus, epithalamus and regions in the midbrain showed greater activation during stop error (SE) as compared to go success (G) trials. BOLD contrasts were overlaid on a structural image in sagittal sections. (b) The ventrolateral prefrontal cortex showed greater activation during post-error go trials with RT slowing (pSEi) as compared to post-error go trials without RT slowing (pSEni). BOLD contrasts were overlaid on a structural image in coronal sections. Color bars represent voxel T values.
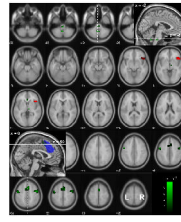
Figure 2.
Brain regions (green) that Granger cause ventrolateral prefrontal cortical (VLPFC, red)
activation during stop signal task. This "causality" map shows the voxel p values superimposed
on a structural image in axial sections. The green scale depicts the statistical significance of
the causality measure (p<0.01, uncorrected). The upper inset shows the cerebellar and pontine
cluster in a sagittal view. The lower inset shows the supplementary motor area or SMA cluster
(green) identified from GCA in sagittal view and its spatial relationship to the anterior cingulate
cortex/SMA cluster identified from general linear modeling (blue). Please see text for further
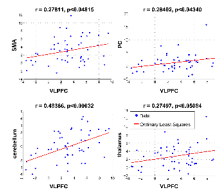explanation.

Figure 3.
Linear correlation between error-related regional activation and ventrolateral prefrontal cortical (VLPFC) activity. Each dot represents one subject. SMA: supplementary motor area; PC: left precentral cortex (PC).
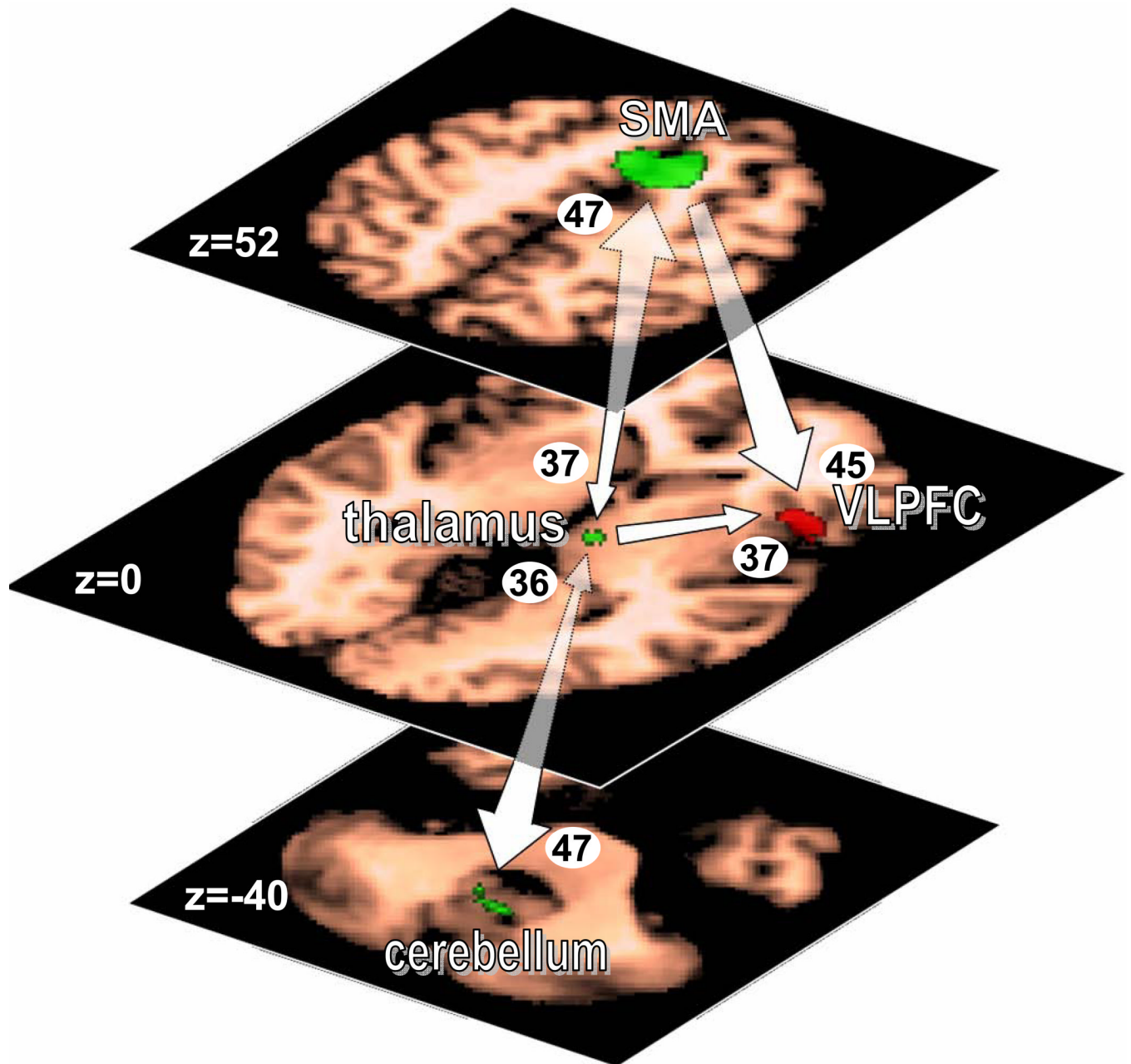
Figure 4.
Multivariate Granger causality analysis of the supplementary motor area (SMA), thalamus, cerebellum and ventrolateral prefrontal cortex (VLPFC). We evaluated for individual subjects whether each of the 12 connections was significant at $p<0.05$, corrected for false discovery rate. Group level statistics was computed using the binomial test with $p<0.01$. The numbers next to the arrow heads represent the number of subjects (out of 54) that show the connection. In the binomial tests, 36 (out of 54) is equivalent to $p<0.00992$; 37: $p<0.00454$; 45: $p<3.64e-7$; and 47: $p<1.15e-8$, respectively.

Table 1

Brain regions that Granger cause ventrolateral prefrontal activation in the stop signal task.

Cluster Size (mm³)	Peak voxel p-value	Peak MNI Coordinate (mm)			Side	Identified region
		x	y	z		
3,656	0.00061	0	8	56	R/L	Supplementary motor area
1,769	0.00151	48	−4	52	R	Middle frontal gyrus/Precentral sulcus
1,392	0.00324	−48	−4	48	L	Middle frontal gyrus/Precentral sulcus
120	0.00697	8	−16	−0	R	Medial thalamus
448	0.00344	0	−28	−40	R/L	Pontine nucleus
608	0.00501	0	−56	−40	L	Cerebellum